Contour Detection of Short Axis Slice
MR Images for Contraction Irregularity Assessment

A Müller[1], A Neitmann[2], N Merkle[3], J Wöhrle[3],
V Hombach[3], HA Kestler[1,2]

[1]Internal Medicine I, University Hospital Ulm, Robert-Koch-Str 8, 89081 Ulm, Germany
[2]Neuroinformatics, University of Ulm, 89069 Ulm, Germany
[3]Dept of Cardiology, University Hospital Ulm, Germany

Abstract

A new method for automatically detecting left ventricular endocardial borders in cardiac MRI short-axis slices was applied to a previously published patient group [1] for which manually drawn contours already existed. An initial point lying in the left ventricular endocardium was found by a size invariant circular Hough transform. A coarse segmentation of the endocardial region was completed by merging surrounding regions and building the convex hull. Adjacent time frames were used to remove jitter from the contour movements. A feature (IRM), extracted from those contours, quantified the irregularities of left ventricular contractions. Patients with dilated cardiomyopathy were separated from the control group by hresholding the IRM parameter.

1.   Introduction

In patients with reduced left ventricular function (LVF) the frequently concomitant left bundle branch block (LBBB) leads to a further deterioration of global heart performance due to asynchronous contraction. Implantation of biventricular pacemakers may be an option for these patients [2]. QRS duration alone has failed to serve as predictive parameter for the clinical outcome of patients after biventricular pacing, since ventricular synchronicity does not necessarily require a synchronous electrical excitation [3]. In previous studies [1], [4] we showed the utility of measuring phase differences in ventricular contours.

Aim of this study was to automatically detect the left ventricular endocardial border in MR images and to develop an irregularity marker similar to those in previous findings [1]. The new marker is exclusively based on the contour of the left ventricular endocardium.

2.   Methods

2.1.   Subject data

The subject group of the previous study [1] was expanded to 20 subjects with dilated cardiomyopathy (DCM) from which 12 had a left bundle branch block (LBBB), and 13 healthy subjects. Due to low image quality and non-uniform brightness distribution two MR recordings had to be excluded from the group of 20 DCM patients.

The remaining 18 DCM patients had an average left ventricular ejection fraction (LVEF) of 27% with standard deviation 8.8%. The control group had an average LVEF of 70% with standard deviation 5.4%.

2.2.   Imaging

Imaging was performed on a $1.5T$ whole body scanner (Intera CV, Philips Medical Systems, Software Release 9.1) with Master Gradients (slew rate $150T/m/s$, amplitude $30mT/m$). A 5-element phased-array cardiac coil was used. Three short survey scans were performed to define position and true axis of the left ventricle. Afterwards, wall motion was imaged during breath holding within long and short-axis slices using a steady-state free precession (balanced fast-field echo) sequence, which provided an excellent endocardial constrast. Cardiac synchronization was achieved by prospective gating. The cine images were recorded with 23 or 32 frames per heart beat and with a slice thickness of $10mm$ ($8mm$ in some cases).

2.3.   Image analysis

All endocardial borders of the left ventricle were manually drawn by an expert (three inner short axis slices) for the whole cardiac cycle using the MASS® plus 5.0 Software (Medis, Leiden, Netherlands). Difficulties in the correct tissue assignment were reduced by observing adjacent slices and time frames in the detection process. The

papillary muscles were assigned to the ventricular cavum. Further data processing was performed with Matlab® 7.04 (MathWorks Inc.).

2.4. Automatic contour detection

The gray valued MR images were streched to the interval $[0, 1]$. The full resolution of the MR images was not necessary for the irregularity computations and was resized to 400 pixels in both dimensions for a higher processing speed. All computations - if not otherwise mentioned - were performed on a single slice.

2.4.1. Finding the left ventricle

A point in the left ventricular endocardium was located by a size invariant circular Hough transform on the first time frame ($t = 1$). The found point selected a region on the previously segmented image. The bounding box of those region lead to a rectangle - the region of interest (ROI) - which enclosed the left ventricle. The same ROI was used for all other time frames $t = 1 \ldots T$, which was a reasonable choice since the first time frame corresponded to the heart in its relaxed state before contraction.

After smoothing the image with a Gaussian lowpass filter ($w = 63$ and $\sigma = 12.5$) the edges were detected by the Canny operator [5]. In addition to that the gradients were computed on the smoothed image with a Sobel differentiator (e.g. [6]). A radius independent circular Hough transform (CHT) (compare e.g. [7], [8], [9]) lead to a point $\mathbf{p}_0$ in the left ventricular endocardium by the median taken independently over the x and y coordinates of the 5 largest accumulator entries. A two-dimensional Hough accumulator was used for the circle centers; the radii were not necessary for this task. Height and width of the accumulator were both reduced to 1/4-th of the image size. At each edge point the gradient defined a line along which the accumulator was incremented (see Fig. 1). To reduce the influence of points near the image border (we assumed that the left ventricle is positioned well) the accumulator increment was chosen to be depending on the pixel position (x, y): $w(x, y) = \exp\left\{-\frac{1}{2}\left(\alpha\frac{x - n_x/2}{n_x/2}\right)^2 - \frac{1}{2}\left(\alpha\frac{y - n_y/2}{n_y/2}\right)^2\right\}$ where n_x and n_y are width and height of the image respectively. In this study we used $\alpha = 1$.

Only the relevant regions were leftover after segmenting the whole image with a global threshold (Otsus method [10]) and a subsequent morphological opening (10 pixels radius, circular shape).

The connected region which enclosed the previously found point $\mathbf{p}_0$ was selected as main region $\mathbf{R}_0$ for the left ventricle. The final ROI was determined by expanding the bounding box of $\mathbf{R}_0$ by a constant factor (1.3) in each
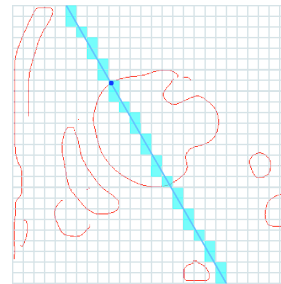

Figure 1. The illustration shows an edge image together with the 2d Hough accumulator (grid). The gradient at the marked edge point (x, y) (small circle in the figure) defines a line along which all accumulator entries are incremented (blue shaded accumulator cells) by the value $w(x, y)$ (see text).

direction. This method successfully selected the rectangle containing the left ventricle for all datasets in this study.

2.4.2. Completing the contour

For each frame $t = 1 \ldots T$ the following procedure was repeated and lead to a first estimate of the left ventricular endocardial pixel set:
1. Clip the image to the ROI.
2. Segment the image with Otsus method.
3. Apply a weak morphological opening (circular shape, radius 1 pixel) to remove noisy structures.
4. Select the region $\mathbf{R}_t$ which covers the point $\mathbf{p}_{t-1}$.
5. Compute the center of gravity $\mathbf{p}_t$ of $\mathbf{R}_t$.
6. Compute the convex hull $\mathbf{H}_t$ of $\mathbf{R}_t$.
7. Interpolate the line segments of $\mathbf{H}_t$ with a circular shaped interpolation $r_c(\theta)$ (see below). After the interpolation the resuling polygon $\mathbf{C}_t$ had at least 256 points.
8. Merge $\mathbf{R}_t$ with other surrounding regions if they build an intersection with $\mathbf{C}_t$ and have less than 5% of the area of $\mathbf{R}_t$ (all regions are filled before estimating its areas by the pixel counts). The resulting region $\mathbf{R}_t'$ is expanded with a repetition of steps 6 and 7 to get the unfiltered contour $\mathbf{R}_t''$.

The endocardial region $\mathbf{R}_t$ was always selected by the center of the preceding main region $\mathbf{R}_{t-1}$, except for the first frame $t = 1$ where the point $\mathbf{p}_0$, found by the circular Hough transform, selected the region. Papillary muscles near the ventricular border lead sometimes to topologically disconnected regions in the segmented image. In those cases the convex hull of $\mathbf{R}_t$ had long line segments clipping parts of the ventricle. The above method tries to merge isolated regions in order to complete the endocardial contour. The pre-information that the left ventricle is circular shaped was reflected by using the parametric curve $r_c(\theta) = \frac{\theta_2 - \theta_1}{r_2 - r_1}(\theta - \theta_1) + r_1$ ($\theta_1 \leq \theta \leq \theta_2$) for interpolating the line segments of the convex hull. Each segment was represented by two polar coordinates (θ_1, r_1)

and (θ_2, r_2) for $\theta_1 \leq \theta_2$ with the mean center of gravity $\mathbf{m}$ (taken over all time frames) as origin of the coordinate system. If $r_1 = r_2$ the curve reduces to a circle segment - otherwise the curve represents the segment of an Archimedic spiral.

Further improvements could be done after this step to acquire a higher contour precision. A multiseeded segmentation approach [11] with seed points based on the previously found contour was not able to improve the contour accuracy.

2.4.3. Continuity correction

Discontinuities of the contour motions were improved by the use of adjacent time frames. Hereto every contour $\mathbf{R}_t''$, $t = 1 \ldots T$ was sampled at the angles $\theta_k = 2\pi \frac{k}{n}$, $k = 0 \ldots n - 1$ for $n = 128$ to give radius profiles $r_k(t) > 0$. This was done by finding the intersection point $\mathbf{m} + r_k(t) \begin{bmatrix} \cos(\theta_k) & \sin(\theta_k) \end{bmatrix}^T$ for all n equiangular rays $k = 0 \ldots n - 1$ originating from the mean contour center $\mathbf{m}$ (taken over all time frames of this slice) with the polygon $\mathbf{R}_t''$. Each time signal $r_k(t)$ for $k = 0 \ldots n - 1$ was independently filtered by a median filter (window size $w = 3$) so that the filtered signals became $r_k'(t) = \mathrm{median}\{r_k(t - \frac{w-1}{2}) \ldots r_k(t + \frac{w-1}{2})\}$ with $r_k(t) = 0$ for $t < 1$ or $t > T$.

Outliers, where the contour of a single time frame was erroneous (if e.g. due to a bad segmentation, the endocardial region became spuriously connected to a region outside the endocardium), could be removed successfully with this method. In the last step each contour $(x_k, y_k)_1^\ell$ (transformed back into cartesian coordinates) was smoothed independently by a periodic moving average filter ($w = 11$) so that the final contour became $\hat{x}_k = \frac{1}{2w+1} \sum_{k-(w-1)/2}^{k+(w-1)/2} x_k$ and $\hat{y}_k = \frac{1}{2w+1} \sum_{k-(w-1)/2}^{k+(w-1)/2} y_k$ whereas $x_k = x_{\ell-k}$ for $k < 1$ and $x_k = x_{k-\ell}$ for $k > \ell$ and similar for y_k.

2.5. A measure of irregularity

In the following we propose a feature which quantifies the irregularity of the movements of the left ventricle given a set of endocardial contours. The marker is required to be low for even radial movements and high for uneven movements. Since the described method extracts only the left ventricular contour from the MR images we adapted our previous method [1] to work on single contours. The reference point, which was previously defined by the right ventricular contour, is now replaced by an equiangular sampling of the left ventricular contour: For each time frame $t = 1 \ldots T$ the contour was reduced to $N = 8$ equiangular distances as described in the previous subsection. The radii $r_1(t) \ldots r_N(t)$ form N time signals.

For all $N(N-1)/2$ signal pairs the (weighted) phase shifts $\mathcal{P} = \{w_{ij}\Phi(u_i, u_j) \mid 1 \leq i < j \leq N\}$ were estimated by the angular distance

$$\Phi(u(t), v(t)) = \arccos\left\{ \frac{\langle u(t) - \overline{u}, v(t) - \overline{v} \rangle}{\|u(t) - \overline{u}\| \cdot \|v(t) - \overline{v}\|} \right\} \quad .$$

The weights $w_{ij} \in [0, 1]$ were defined as

$$w_{ij} = \Lambda\left(\left(\frac{|i - j|}{\lfloor n/2 \rfloor} \mod 2 \right) - 1 \right)$$

with the triangle function

$$\Lambda(x) = \begin{cases} 1 - |x| & \text{for } |x| \leq 1 \\ 0 & \text{otherwise} \end{cases}$$

and $x \mod m$ the modulo function defined for real numbers x and m. The weighting gave a stronger influence of phase differences between opposite cardial borders (e.g. a_1 and $a_{\lfloor N/2 \rfloor}$) rather than motions between neighbour signals (e.g. a_1 and a_2). For each slice the median of $\mathcal{P}$ was taken as irregularity measure which was then averaged over the three inner slices to acquire the final IRM value.

3. Results

The described automatic contour detection method lead with the proposed asynchronicity marker IRM to the separability of DCM patients from the control group by a single threshold value (see figure 2 left). Furthermore the IRM values of the automatically detected contours were compared to those extracted from the manually detected contours (see figure 2 right). There was a slight bias with a mean phase difference of $+0.044$ towards the manual contours.

4. Discussion and conclusions

A fast method for automatically tracing the left ventricular endocardial border in cardiac MRI was proposed. It was shown that the developed feature (IRM) successfully quantified the asynchronicity of cardiac movements and may be a promising marker for the detection of dilated cardiomyopathy (DCM).

The automatic contour detection may be improved to give more accurate contours for difficult MR images (especially those concerning large papillary muscles at the ventricular), though, for the assessment of the ventricular asynchronicity, a higher contour accuracy was not necessary as could be shown by comparing the irregularity markers extracted from automatically detected contours with those extracted from manually drawn contours.
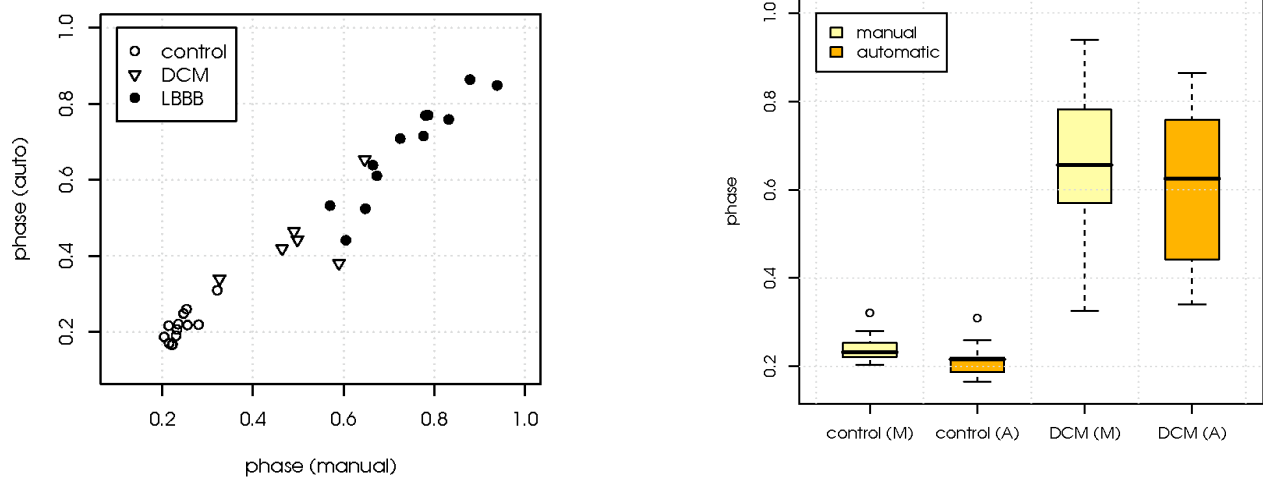
Figure 2. The left diagram shows a scatter plot with the IRM phase values for the manually detected contours (x-axis) and for the automatically detected contours (y-axis). The DCM group was separable from the control group by a single threshold. The right diagram shows boxplots of the IRM phase values for the DCM patients and the control group for both contour detection methods (A=automatic detection, M=manual detection)..

Acknowledgements

References

[1] Müller A, Merkle N, Hombach V, Grebe O, Nusser T, Wöhrle J, Binner L, Kestler HA. Extracting robust features from cardiac magnetic resonance image contours for detecting dilated cardiomyopathy. In Computers in Cardiology, volume 31. IEEE, 2004; 157–160.

[2] Cazeau S, Leclercq C, Lavergne T, Walker S, Varma C, Linde C, Garrigue S, Kappenberger L, Haywood GA, Santini M, Bailleul C, Daubert JC. Effects of multisite biventricular pacing in patients with heart failure and intraventricular conduction delay. N Engl J Med 2001;344(12):873–880.

[3] Leclercq C, Faris O, Tunin R, Johnson J, Kato R, Evans F, Spinelli J, Halperin H, McVeigh E, Kass DA. Systolic improvement and mechanical resynchronization does not require electrical synchrony in the dilated failing heart with left bundle-branch block. Circ 2002;106(14):1760–1763.

[4] Grebe O, Müller A, Merkle N, Wöhrle J, Binner L, Höher M, Hombach V, Neumann H, Kestler HA. Estimation of intra- and inter-ventricular dyssynchronization with cardiac magnetic resonance imaging. In Computers in Cardiology, volume 30. IEEE, 2003; 741–743.

[5] Canny J. A computational approach to edge detection. IEEE Trans on PAMI 1986;8(6):679–698.

[6] Jähne B. Digitale Bildverarbeitung. Springer, 1997.

[7] Kimme C, Ballard D, Sklansky J. Finding circles by an array of accumulators. Commun ACM 1975;18(2):120–122.

[8] Atherton TJ, Kerbyson DJ. Size invariant circle detection. Image Vision Comput 1999;17(11):795–803.

[9] Kälviäinen H, Hirvonen P, Xu L, Oja E. Probabilistic and non-probabilistic hough transforms: overview and comparisons. Image and Vision Computing 1995;13(4):239–252.

[10] Otsu N. A threshold selection method from gray-level histograms. IEEE Transactions on Systems Man and Cybernetics 1979;9(1):62–66.

[11] Herman GT, Carvalho BM. Multiseeded segmentation using fuzzy connectedness. IEEE Transactions on Pattern Analyiss and Machine Intelligence 2001;23(5):460–474.

Address for correspondence:

Hans A. Kestler
University of Ulm
Internal Medicine I
Robert-Koch-Str. 8
89081 Ulm, Germany
hans.kestler@uniklinik-ulm.de